

1 **Flip Distance Between Triangulations of a Simple Polygon is**
2 **NP-Complete**

3 **Oswin Aichholzer · Wolfgang Mulzer ·**
4 **Alexander Pilz**

5
6 the date of receipt and acceptance should be inserted later

7 **Abstract** Let T be a triangulation of a simple polygon. A *flip* in T is the operation
8 of replacing one diagonal of T by a different one such that the resulting graph is again
9 a triangulation. The *flip distance* between two triangulations is the smallest number
10 of flips required to transform one triangulation into the other. For the special case of
11 convex polygons, the problem of determining the shortest flip distance between two
12 triangulations is equivalent to determining the rotation distance between two binary
13 trees, a central problem which is still open after over 25 years of intensive study.

14 We show that computing the flip distance between two triangulations of a simple
15 polygon is NP-hard. This complements a recent result that shows APX-hardness of
16 determining the flip distance between two triangulations of a planar point set.

O. Aichholzer and A. Pilz are supported by the ESF EUROCORES programme EuroGIGA - ComPoSe, Austrian Science Fund (FWF): I 648-N18. W. Mulzer is supported in part by DFG project MU/3501/1. Part of this work was done while A. Pilz was recipient of a DOC-fellowship of the Austrian Academy of Sciences at the Institute for Software Technology, Graz University of Technology, Austria. Preliminary versions appeared as O. Aichholzer, W. Mulzer, and A. Pilz, *Flip Distance Between Triangulations of a Simple Polygon is NP-Complete* in Proc. 29th EuroCG, pp. 115–118, 2013, and in Proc. 21st ESA, pp. 13–24, 2013 [2, 3].

O. Aichholzer · A. Pilz (✉)

Institute for Software Technology, Graz University of Technology, Austria.

Tel.: +43-316-873-5732

Fax: +43-316-873-5706

E-mail: [oach|apilz]@ist.tugraz.at

W. Mulzer

Institut für Informatik, Freie Universität Berlin, Germany.

E-mail: mulzer@inf.fu-berlin.de

17 **Keywords** triangulations · flip distance · simple polygon

18 **Mathematics Subject Classification (2000)** 68U05

19 **1 Introduction**

20 Let P be a simple polygon in the plane, that is, a closed region bounded by a piece-
21 wise linear, simple cycle. A *triangulation* of P is a geometric (straight-line) maximal
22 outerplanar graph whose outer face is the complement of P and whose vertex set consists
23 of the vertices of P . The edges that are not on the outer face are called *diagonals*. Let d
24 be a diagonal whose removal creates a convex quadrilateral. Replacing d with the other
25 diagonal of the quadrilateral yields another triangulation of P . This operation is called
26 a *flip*. The *flip graph* of P is the abstract graph whose vertices are the triangulations
27 of P and in which two triangulations are adjacent if and only if they differ by a single
28 flip. We study the *flip distance*, i.e., the minimum number of flips required to transform
29 a given source triangulation into a target triangulation.

30 Edge flips became popular in the context of Delaunay triangulations. Lawson [15]
31 proved that any triangulation of a planar n -point set can be transformed into any other
32 by $O(n^2)$ flips. Hence, for every planar n -point set the flip graph is connected with diam-
33 eter $O(n^2)$. Later, Lawson showed that in fact every triangulation can be transformed
34 to the Delaunay triangulation by $O(n^2)$ flips that locally fix the Delaunay property [16].
35 Hurtado, Noy, and Urrutia [11] gave an example where the flip distance is $\Omega(n^2)$, and
36 they showed that the same bounds hold for triangulations of simple polygons. They
37 also proved that if the polygon has k reflex vertices, then the flip graph has diameter
38 $O(n + k^2)$. In particular, the flip graph of any planar polygon has diameter $O(n^2)$. Their
39 result also generalizes the well-known fact that the flip distance between any two tri-
40 angulations of a convex polygon is at most $2n - 10$, for $n > 12$. This was shown by
41 Sleator, Tarjan, and Thurston [22] in their work on the flip distance in convex poly-
42 gons. The latter case is particularly interesting due to the correspondence between flips
43 in triangulations of convex polygons and rotations in binary trees: The dual graph of
44 such a triangulation is a binary tree, and a flip corresponds to a rotation in that tree;
45 conversely, for every binary tree, a triangulation can be constructed.

46 We mention two further remarkable results on flip graphs for point sets. Hanke,
47 Ottmann, and Schuierer [10] showed that the flip distance between two triangulations is

48 bounded by the number of crossings in their overlay. Eppstein [9] gave a polynomial-time
49 algorithm for calculating a lower bound on the flip distance. His bound is tight for point
50 sets with no empty 5-gons; however, except for small instances, such point sets are not
51 in general position (i.e., they must contain collinear triples) [1]. A recent survey on flips
52 is provided by Bose and Hurtado [4].

53 Recently, the problem of finding the flip distance between two triangulations of a
54 point set was shown to be NP-hard by Lubiw and Pathak [18] and, independently, by
55 Pilz [19]. The latter proof was later improved to show APX-hardness of the problem. A
56 recent preprint shows that the problem is fixed-parameter tractable [14]. Here, we show
57 that the corresponding problem remains NP-hard even for simple polygons. This can
58 be seen as a further step towards settling the complexity of deciding the flip distance
59 between triangulations of convex polygons or, equivalently, the rotation distance between
60 binary trees. This variant of the problem was probably first addressed by Culik and
61 Wood [7] in 1982 (showing a flip distance of $2n - 6$) in the context of similarity measures
62 between trees.

63 We now give the formal problem definition: given a simple polygon P , two triangula-
64 tions T_1 and T_2 of P , and an integer l , decide whether T_1 can be transformed into T_2 by
65 at most l flips. We call this decision problem POLYFLIP. To show NP-hardness, we give
66 a polynomial-time reduction from the problem RECTILINEAR STEINER ARBORESCENCE
67 to POLYFLIP. RECTILINEAR STEINER ARBORESCENCE was shown to be NP-hard by Shi
68 and Su [21]. In Section 2, we describe the problem in detail. We present the well-known
69 *double chain* (used by Hurtado, Noy, and Urrutia [11] for giving their lower bound), a
70 major building block in our reduction, in Section 3. Finally, in Section 4, we describe
71 our reduction and prove that it is correct.

72 2 The Rectilinear Steiner Arborescence Problem

73 Let S be a set of N points in the plane whose coordinates are nonnegative integers.
74 The points in S are called *sinks*. A *rectilinear tree* A is a connected acyclic collection of
75 horizontal and vertical line segments that intersect only at their endpoints. The *length*
76 of A is the total length of all segments in A (cf. [13, p. 205]). The tree A is a *rectilinear*
77 *Steiner tree* for S if every sink in S appears as an endpoint of a segment in A . We call A
78 a *rectilinear Steiner arborescence* (RSA) for S if (i) A is rooted at the origin; (ii) every

79 leaf of A lies at a sink in S ; and (iii) for each $s = (x_s, y_s) \in S$, the length of the path
 80 in A from the origin to s equals $x_s + y_s$, i.e., all edges in A point north or east, as seen
 81 from the origin [20]. In the problem RECTILINEAR STEINER ARBORESCENCE, we are
 82 given a set of sinks S and an integer k . The question is whether there is an RSA for S
 83 of length at most k . Shi and Su showed that RECTILINEAR STEINER ARBORESCENCE
 84 is strongly NP-complete; in particular, it remains NP-complete if S is contained in an
 85 $n \times n$ grid, with n polynomially bounded in N , the number of sinks [21].¹

86 We will need the following important structural property of the RSA. Let A be an
 87 RSA for a set S of sinks. Let e be a vertical segment in A that does not contain a sink.
 88 Suppose there is a horizontal segment f incident to the upper endpoint a of e . Since A
 89 is an arborescence, a is the left endpoint of f . Suppose further that a is not the lower
 90 endpoint of another vertical edge. Take a copy e' of e and translate it to the right until e'
 91 hits a sink or another segment endpoint (this will certainly happen at the right endpoint
 92 of f); see Fig. 1. The segments e and e' define a rectangle R . The upper and left side of R
 93 are completely covered by e and (a part of) f . Since a has only two incident segments,
 94 every sink-root path in A that goes through e or f contains these two sides of R , entering
 95 the boundary of R at the upper right corner d and leaving it at the lower left corner b .
 96 We reroute every such path at d to continue clockwise along the boundary of R until it
 97 meets A again (this certainly happens at b), and we delete e and the part of f on R .
 98 In the resulting tree we subsequently remove all unnecessary segments (this happens if
 99 there are no more root-sink paths through b) to obtain another RSA A' for S . Then A'
 100 is not longer than A . This operation is called *sliding e to the right*. If similar conditions
 101 apply to a horizontal edge, we can *slide it upwards*. The *Hanan grid* for a point set is
 102 the set of all vertical and horizontal lines through its points. Through repeated segment
 103 slides in a shortest RSA, one can obtain the following theorem.

104 **Theorem 2.1** ([20]) *Let S be a set of sinks. There is a minimum-length RSA A for S*
 105 *such that all segments of A are on the Hanan grid for $S \cup \{(0, 0)\}$.* □

106 We use a restricted version of RECTILINEAR STEINER ARBORESCENCE, called YRSA.
 107 An instance (S, k) of YRSA differs from an instance for RECTILINEAR STEINER AR-
 108 BORESCENCE in that we require that no two sinks in S have the same y -coordinate.

109 **Theorem 2.2** *YRSA is strongly NP-complete.*

¹ Although a polynomial-time algorithm was claimed [23], it has later been shown to be incorrect [20].

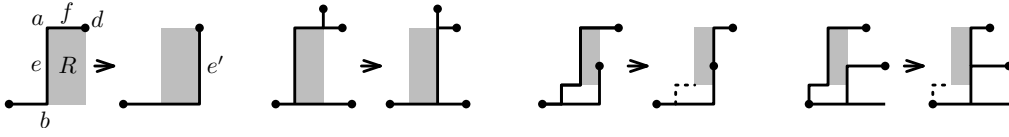


Fig. 1 The slide operation. The dots depict sinks; the rectangle R is drawn gray. The dotted segments are deleted, since they do no longer lead to a sink.

110 *Proof* Due to Theorem 2.1, YRSA and RECTILINEAR STEINER ARBORESCENCE are in
 111 NP [21]. We now show how to transform an instance (S, k) of RECTILINEAR STEINER
 112 ARBORESCENCE to an instance of YRSA. We may assume that $N = |S| \geq 3$, and we
 113 number the sinks as $S = \langle s_1, s_2, \dots, s_N \rangle$ in an arbitrary fashion. For $i = 1, \dots, N$,
 114 let (x_i, y_i) be the coordinates of s_i and define $s'_i := (x_i N^4, y_i N^4 + i)$. We set $S' :=$
 115 $\{s'_1, s'_2, \dots, s'_N\}$. The y -coordinates of the sinks in S' are pairwise distinct. We will show
 116 that there is an RSA for S of length at most k if and only if there is an RSA for S' of
 117 length at most $kN^4 + N^3$.

118 Let A be a rectilinear Steiner arborescence for S of length at most k . We scale A by
 119 N^4 and draw a vertical segment from each leaf to the sink in S' above it. This gives an
 120 RSA for S' of length at most $kN^4 + N^2 < kN^4 + N^3$.

121 Conversely, let A' be an RSA for S' of length at most $kN^4 + N^3$. Due to Theorem 2.1,
 122 we can assume that A' is on the Hanan grid. We round the y -coordinate of every segment
 123 endpoint in A' down to the next multiple of N^4 (possibly removing segments of length 0).
 124 The resulting drawing remains connected; every path to the origin remains monotone;
 125 and since the segments of A' lie on the Hanan grid of $S' \cup \{(0, 0)\}$, no new cycles are
 126 introduced. Thus, the resulting drawing constitutes an arborescence A'' for the set S''
 127 of sinks obtained by scaling S by N^4 . Since A' lies on the Hanan grid, it is a union
 128 of N paths, each with at most N vertical segments. The rounding operation increases
 129 the length of each such vertical segment by at most N . Thus, the total length of A'' is
 130 at most $kN^4 + 2N^3$. By Theorem 2.1 there exists an optimum arborescence A^* for S''
 131 that lies on the Hanan grid. The length of A^* is a multiple of N^4 , and thus at most
 132 kN^4 , since $2N^3 < N^4$ for $N \geq 3$. It follows that S has an RSA of length at most k .

133 Therefore, (S, k) is a yes-instance for RECTILINEAR STEINER ARBORESCENCE if and
 134 only if $(S', kN^4 + N^3)$ is a yes-instance for YRSA. Since $(S', kN^4 + N^3)$ can be computed
 135 in polynomial time from (S, k) , and since the coordinates in S' are polynomially bounded
 136 in the coordinates of S , it follows that YRSA is strongly NP-complete. \square

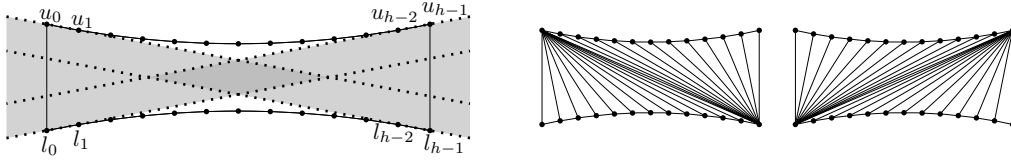


Fig. 2 Left: The polygon and the hourglass (gray) of a double chain. The diamond-shaped flip-kernel can be extended arbitrarily by flattening the chains. Right: The upper extreme triangulation T_u and the lower extreme triangulation T_l .

137 Due to Theorem 2.1, we get the following technical corollary, which will be useful
138 later.

139 **Corollary 2.3** *YRSA remains strongly NP-complete even if the sinks have coordinates*
140 *that are a multiple of a positive integer whose value is polynomial in N .*

141 3 Double Chains

142 Our definitions (and illustrations) follow [19]. A *double chain* D is a polygon that con-
143 sists of two chains, an *upper chain* and a *lower chain*. There are h vertices on each chain,
144 $\langle u_0, \dots, u_{h-1} \rangle$ on the upper chain and $\langle l_0, \dots, l_{h-1} \rangle$ on the lower chain, both numbered
145 from left to right, and D is defined by $\langle l_0, \dots, l_{h-1}, u_{h-1}, \dots, u_0 \rangle$. Any point on one chain
146 sees every point on the other chain, and any quadrilateral formed by three vertices of
147 one chain and one vertex of the other chain is non-convex; see Fig. 2 (left). We call the
148 triangulation T_u of D where u_0 has maximum degree the *upper extreme triangulation*;
149 observe that this triangulation is unique. The triangulation T_l of D where l_0 has max-
150 imum degree is called the *lower extreme triangulation*. The two extreme triangulations
151 are used to show that the diameter of the flip graph is quadratic; see Fig. 2 (right).

152 **Theorem 3.1 (Hurtado, Noy, Urrutia [11])** *The flip distance between T_u and T_l*
153 *is $(h - 1)^2$. \square*

154 Through a slight modification of D , we can make the flip distance between the upper
155 and the lower extreme triangulation linear. This will enable us in our reduction to impose
156 a certain structure on short flip sequences. To describe this modification, we first define
157 the *flip-kernel* of a double chain.

158 Let W_1 be the wedge defined by the lines through u_0u_1 and l_0l_1 whose interior
159 contains no vertex of D but intersects the segment u_0l_0 . Define W_h analogously by the

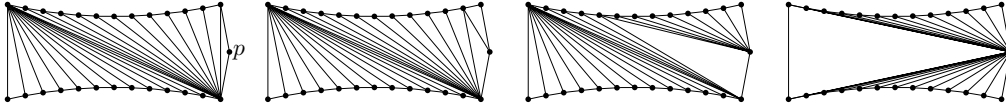


Fig. 3 The extra point p in the flip-kernel of D allows flipping one extreme triangulation of Q to the other in $4h - 4$ flips.

160 lines through $u_{h-1}u_{h-2}$ and $l_{h-1}l_{h-2}$. We call $W := W_1 \cup W_h$ the *hourglass* of D . The
 161 unbounded set $W \cup D$ is defined by four rays and the two chains. The *flip-kernel* of D is
 162 the intersection of the four closed half-planes below the lines through u_0u_1 and $u_{h-2}u_{h-1}$
 163 and above the lines through l_0l_1 and $l_{h-2}l_{h-1}$.²

164 **Definition 3.2** Let D be a double chain and let p be a point in the flip-kernel
 165 of D to the right of the directed line $l_{h-1}u_{h-1}$. The polygon given by the sequence
 166 $\langle l_0, \dots, l_{h-1}, p, u_{h-1}, \dots, u_0 \rangle$ is called a *double chain extended by p* . The upper and the
 167 lower extreme triangulation of such a polygon contain the edge $u_{h-1}l_{h-1}$ as a diagonal
 168 and are otherwise defined in the same way as for D .

169 The flip distance between the two extreme triangulations of D extended by a point p
 170 is much smaller than for D [24]. Fig. 3 shows how to transform them into each other
 171 with $4h - 4$ flips. The next lemma shows that this is optimal, even for more general
 172 polygons. The lemma is a slight generalization of a lemma by Lubiw and Pathak [18] on
 173 double chains of constant size.

174 **Lemma 3.3** Suppose that $h \geq 5$ and consider a polygon that contains D and has
 175 $\langle l_0, \dots, l_{h-1} \rangle$ and $\langle u_{h-1}, \dots, u_0 \rangle$ as part of its boundary. Let T_1 and T_2 be two triangula-
 176 tions that contain the upper extreme triangulation and the lower extreme triangulation
 177 of D as a sub-triangulation, respectively. Then T_1 and T_2 have flip distance at least
 178 $4h - 4$.

179 *Proof* We slightly generalize a proof by Lubiw and Pathak [18] for double chains of
 180 constant size.

181 Let C_u be the upper chain and C_l be the lower chain of D . The triangulation T_1 has
 182 $2(h - 1)$ triangles with an edge on C_u or on C_l . These triangles are called *anchored*, and
 183 the vertex not incident to the edge on C_u or on C_l is called the *apex*. For each anchored
 184 triangle with an edge on C_u , the apex must move from l_{h-1} to l_0 , and similarly for C_l .

² The flip-kernel of D might not be completely inside the polygon D . This is in contrast to the “visibility kernel” of a polygon.

185 We distinguish three types of flips depending on whether the convex quadrilateral whose
 186 diagonal is flipped has (1) four; (2) three; or (3) at most two vertices on D . A flip of
 187 type (1) moves the apex of two anchored triangles by one; a flip of type (2) moves the
 188 apex of one anchored triangle from D to a point outside D or back again; and a flip of
 189 type (3) does not move any apex of an anchored triangle along D or between a vertex
 190 of D and a vertex not in D .

191 We say that an anchored triangle is of type (1) if its apex is moved only by flips of
 192 type (1). It is of type (2) if its apex is moved by at least one flip of type (2). Every
 193 anchored triangle is either of type (1) or of type (2). A type (1) triangle must be involved
 194 in at least $h - 1$ flips of type (1), and each of these flips can affect at most one other
 195 type (1) triangle. A type (2) triangle must be involved in at least 2 flips of type (2), and
 196 each of these flips can affect no other anchored triangle. Thus, if we have m_1 type (1)
 197 triangles and m_2 type (2) triangles, we need at least $(h - 1)m_1/2 + 2m_2$ flips. For $h \geq 5$,
 198 we have $(h - 1)m_1/2 + 2m_2 \geq 2(m_1 + m_2) = 4h - 4$, as claimed. \square

199 The following result can be seen as a special case of [19, Proposition 1].

200 **Lemma 3.4** *Consider a polygon that contains D and has $\langle u_{h-1}, \dots, u_0, l_0, \dots, l_{h-1} \rangle$ as
 201 part of its boundary. Let T_1 and T_2 be two triangulations that contain the upper and
 202 the lower extreme triangulation of D as a sub-triangulation, respectively. Let σ be a flip
 203 sequence from T_1 to T_2 such that there is no triangulation in σ containing a triangle
 204 with one vertex at the upper chain, the other vertex at the lower chain, and the third
 205 vertex at a point in the interior of the hourglass of D . Then $|\sigma| \geq (h - 1)^2$.*

206 *Proof* Our reasoning is similar to the proof of Lemma 3.3, see also [18]. As before, let
 207 C_u and C_l be the upper and lower chain of D , and call a triangle with an edge on C_u or
 208 on C_l *anchored*, the third vertex being the *apex*. Any triangulation of the given polygon
 209 has $2(h - 1)$ anchored triangles.

210 We will argue that for each triangulation of σ there exists a line ℓ that separates
 211 C_u from C_l and that intersects all anchored triangles. This is clear if the apices of
 212 all anchored triangles lie on the other chain or outside the hourglass. Now consider a
 213 triangulation of the sequence σ where at least one anchored triangle has its apex at a
 214 vertex v inside the hourglass. Let r be a ray that starts at a point on u_0l_0 and passes
 215 through v such that the supporting line of r separates C_u from C_l (such a ray must
 216 exist since v is inside the hourglass). Then r intersects at least one triangle that is not

217 anchored, because the triangle whose interior is intersected by r before reaching v cannot
 218 be anchored. Let Δ be the first non-anchored triangle whose interior is intersected by r .
 219 Then Δ has one vertex on C_u and one vertex on C_l . By assumption, the third vertex
 220 of Δ cannot be inside the hourglass, so it must lie outside. This means that one of the
 221 vertices of Δ has to be either u_{h-1} or l_{h-1} . This implies that either all anchored triangles
 222 at C_u or all anchored triangles C_l , respectively, have their apex at the opposite chain.
 223 Thus, also for this triangulation there exists a line ℓ that separates C_u from C_l and that
 224 intersects all anchored triangles. Observe that every such line intersects the anchored
 225 triangles in the same order.

226 Now we proceed similarly as in the proof of Hurtado, Noy, and Urrutia [11]: we
 227 observe that an anchored triangle at C_u and an anchored triangle at C_l can change their
 228 relative position along ℓ only if they have an edge in common and this edge is flipped.
 229 This results in an overall number of $(h-1)^2$ flips. \square

230 4 The Reduction

231 We reduce YRSA to POLYFLIP. Let S be a set of N sinks. By Corollary 2.3, we can
 232 assume that the coordinates of sinks of S are multiples of a factor $\beta = 2N$ in $\{0, \dots, \beta n\}$.
 233 Further, we can restrict ourselves to YRSA instances of the form $(S, \beta k)$. Thus, we
 234 imagine that the sinks are embedded on a $\beta n \times \beta n$ grid. The reasons for the choice of β
 235 will become clear below.

236 We construct a polygon P and two triangulations T_1, T_2 in P such that a shortest
 237 flip sequence from T_1 to T_2 corresponds to a shortest RSA for S . To this end, we will
 238 describe how to interpret any triangulation of P as a *chain path*, a path in the integer
 239 grid that starts at the root and uses only edges that go north or east. It will turn out
 240 that flips in P essentially correspond to moving the endpoint of the chain path along the
 241 grid. We choose P, T_1 , and T_2 in such a way that a shortest flip sequence between T_1 and
 242 T_2 moves the endpoint of the chain path according to an Eulerian traversal of a shortest
 243 RSA for S . To force the chain path to visit all sinks, we use the observations from
 244 Section 3: the polygon P contains a double chain for each sink, so that only for certain
 245 triangulations of P it is possible to flip the double chain quickly. These triangulations will
 246 be exactly the triangulations that correspond to the chain path visiting the appropriate
 247 sink. To force the sinks to be visited, we, with foresight, fix the number of points in

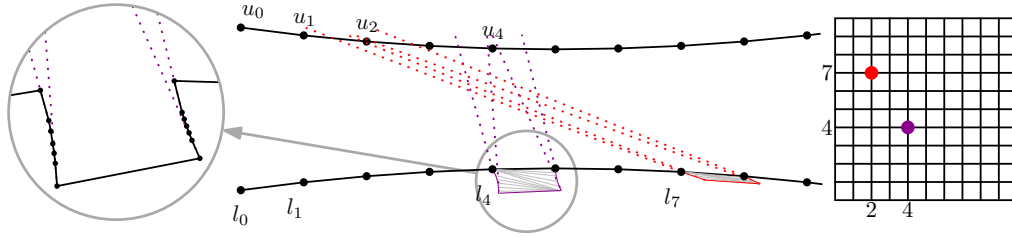


Fig. 4 The sink gadget for a sink (x_s, y_s) is obtained by replacing the edge $l_{y_s} l_{y_s+1}$ by a double chain with d vertices on each chain. The double chain is oriented such that u_{x_s} is the only point inside its hourglass and its flip-kernel.

248 each of the two chains of a double chain representing a sink to $d = nN$ (recall that n is
 249 polynomial in N).

250 4.1 The Construction

251 We take a double chain D with $\beta n + 2$ vertices on each chain such that the flip-kernel
 252 of D extends to the right of $l_{\beta n+1} u_{\beta n+1}$. We add a point z to that part of the flip-kernel,
 253 and we let Q be the polygon defined by $\langle l_0, \dots, l_{\beta n+1}, z, u_{\beta n+1}, \dots, u_0 \rangle$, i.e., a double
 254 chain extended by z (recall Definition 3.2). Next, we add double chains to Q in order
 255 to encode the sinks in S . For each sink $s = (x_s, y_s)$, we remove the edge $l_{y_s} l_{y_s+1}$, and
 256 we replace it by a (rotated) double chain D_s with d vertices on each chain, such that l_{y_s}
 257 and l_{y_s+1} become the last point on the lower and the upper chain of D_s , respectively.
 258 We orient D_s in such a way that u_{x_s} is the only point inside the hourglass of D_s and so
 259 that u_{x_s} lies in the flip-kernel of D_s ; see Fig. 4. We refer to the added double chains as
 260 the *sink gadgets*, and we call the resulting polygon P . Since the y -coordinates in S are
 261 pairwise distinct, there is at most one sink gadget per edge of the lower chain of Q . Since
 262 $\beta \geq 2$, no two sink gadgets are placed on neighboring edges of Q , and can be constructed
 263 such that they do not overlap. Hence, P is a simple polygon. The precise placement of
 264 the sink gadgets is flexible, so given an appropriate embedding of D , we can make all
 265 coordinates integers whose value is polynomial in the input size; see Appendix A for
 266 details.

267 Next, we describe the source and target triangulation for P . In the source triangulation
 268 T_1 , the interior of Q is triangulated such that all edges are incident to z . The sink
 269 gadgets are all triangulated with the upper extreme triangulation. The target triangulation

270 tion T_2 is similar, but now the sink gadgets are all triangulated with the lower extreme
271 triangulation.

272 To get from T_1 to T_2 , we must go from one extreme triangulation to the other for
273 each sink gadget D_s . By Lemma 3.4, this requires $(d-1)^2$ flips, unless the flip sequence
274 creates a triangle that allows us to use the vertex in the flip-kernel of D_s . In this case,
275 we say that the flip sequence *visits* the sink s . The main idea is that, since the value
276 chosen for d is large, a shortest flip sequence must visit all sinks, and we will show that
277 this induces an RSA for S of comparable length. Conversely, we will show how to derive
278 a flip sequence from an RSA. The precise statement is given in the following theorem.

279 **Theorem 4.1** *Let $N \geq 3$, and set $\beta = 2N$. Let S be a set of N sinks such that*
280 *the coordinates of the sinks are multiples of β in $\{0, \dots, \beta n\}$, where n is polynomially*
281 *bounded in N . Set $d = nN$ and let P be the simple polygon and T_1 and T_2 the two*
282 *triangulations of P as described above. Then for any $k \geq 1$, the flip distance between T_1*
283 *and T_2 w.r.t. P is at most $2\beta k + (4d - 2)N$ if and only if S has an RSA of length at*
284 *most βk .*

285 We will prove Theorem 4.1 in the following sections. But first, let us show how to
286 use it for our NP-completeness result.

287 **Theorem 4.2** *POLYFLIP is NP-complete.*

288 *Proof* As mentioned in the introduction, the flip distance in polygons is polynomially
289 bounded, so POLYFLIP is in NP. We reduce from YRSA. Let $(S, \beta k)$ be an instance of
290 YRSA as above. We construct P and T_1, T_2 as described above. This takes polynomial
291 time (see Appendix A for details on the coordinate representation). By Theorem 4.1,
292 there exists an RSA for S of length at most βk if and only if there exists a flip sequence
293 between T_1 and T_2 of length at most $2\beta k + (4d - 2)N$. □

294 4.2 Chain Paths

295 Now we introduce the *chain path*, our main tool to establish a correspondence between
296 flip sequences and RSAs. Let T be a triangulation of Q (i.e., the polygon P without the
297 sink gadgets, cf. Section 4.1). A *chain edge* is an edge of T between the upper and the
298 lower chain of Q . A *chain triangle* is a triangle of T that contains two chain edges. Let
299 e_1, \dots, e_m be the chain edges, sorted from left to right according to their intersection

323 **Lemma 4.7** *Any triangulation T of Q uniquely determines a chain path, and vice versa.*
 324 *A flip in T corresponds to one of the following operations on the chain path: (i) move*
 325 *the endpoint b north or east; (ii) shorten the path at b ; (iii) change an east-north bend*
 326 *to a north-east bend, or vice versa. \square*

327 4.3 From an RSA to a Short Flip Sequence

328 Using the notion of a chain path, we now prove the “if” direction of Theorem 4.1.

329 **Lemma 4.8** *Let $k \geq 1$ and A an RSA for S of length βk . Then the flip distance between*
 330 *T_1 and T_2 w.r.t. P is at most $2\beta k + (4d - 2)N$.*

331 *Proof* The triangulations T_1 and T_2 both contain a triangulation of Q whose chain path
 332 has its endpoint b at the root. We use Lemma 4.7 to generate flips inside Q so that b
 333 traverses A in a depth-first manner. This needs $2\beta k$ flips.

334 Each time b reaches a sink s , we move b north. This creates a chain triangle that
 335 allows the edges in the sink gadget D_s to be flipped to the auxiliary vertex in the
 336 flip-kernel of D_s . The triangulation of D_s can then be changed with $4d - 4$ flips; see
 337 Lemma 3.3. Next, we move b back south and continue the traversal. Moving b at s needs
 338 two additional flips, so we take $4d - 2$ flips per sink, for a total of $2\beta k + (4d - 2)N$
 339 flips. \square

340 4.4 From a Short Flip Sequence to an RSA

341 Finally, we consider the “only if” direction in Theorem 4.1. Let τ be a flip sequence on Q .
 342 We say that τ *visits* a sink $s = (x_s, y_s)$ if τ has at least one triangulation that contains
 343 the chain triangle $u_{x_s} l_{y_s} l_{y_s+1}$. We call τ a *flip traversal* for S if (i) τ begins and ends
 344 in the triangulation whose corresponding chain path has its endpoint b at the root and
 345 (ii) τ visits every sink in S . The following lemma shows that every short flip sequence σ
 346 in P can be mapped to a flip traversal (where with “short”, we mean $|\sigma| < (d - 1)^2$).

347 **Lemma 4.9** *Let σ be a flip sequence from T_1 to T_2 w.r.t. P with $|\sigma| < (d - 1)^2$. Then*
 348 *there is a flip traversal τ for S with $|\tau| \leq |\sigma| - (4d - 4)N$.*

349 *Proof* We show how to obtain a flip traversal τ for S from σ . Let T be a triangulation
 350 of P . A triangle of T is an *inner triangle* if all its sides are diagonals. It is an *ear* if two

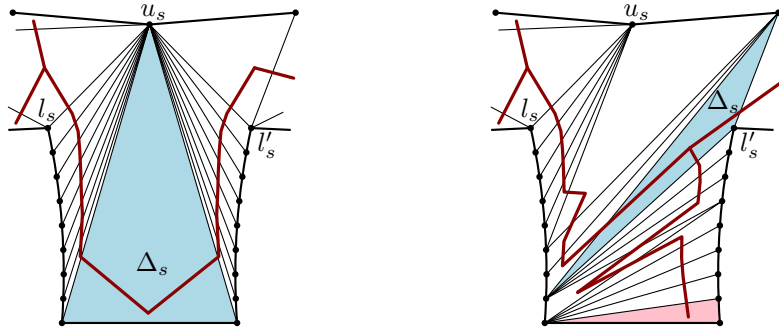


Fig. 6 Triangulations of D_s in P with $\Delta_s = \Delta$ (left), and with Δ being an ear (red) and Δ_s an inner triangle (right). The fat tree indicates the dual.

351 of its sides are polygon edges. By construction, every inner triangle of T must have (i)
 352 one vertex incident to z (the rightmost vertex of Q), or (ii) two vertices incident to a
 353 sink gadget (or both). There can be only one triangle of type (ii) per sink gadget. The
 354 weak (graph theoretic) dual of T is a tree in which ears correspond to leaves and inner
 355 triangles have degree 3.

356 For a sink $s = (x_s, y_s)$, let D_s be the corresponding sink gadget. It lies between
 357 the vertices l_{y_s} and l_{y_s+1} and has exactly u_{x_s} in its flip kernel. For brevity, we will
 358 write l_s for l_{y_s} , l'_s for l_{y_s+1} , and u_s for u_{x_s} . We define a triangle Δ_s for D_s . Consider
 359 the bottommost edge e of D_s , and let Δ be the triangle of T that is incident to e . By
 360 construction, Δ is either an ear of T , or it is the triangle defined by e and u_s . In the
 361 latter case, we set $\Delta_s = \Delta$. In the former case, we claim that T has an inner triangle
 362 Δ' with two vertices on D_s : follow the path from Δ in the weak dual of T ; while the
 363 path does not encounter an inner triangle, the next triangle must have an edge of D_s
 364 as a side. There is only a limited number of such edges, so eventually we must meet an
 365 inner triangle Δ' . We then set $\Delta_s = \Delta'$; see Fig. 6. Note that Δ_s might be $l_s l'_s u_s$.

366 For each sink s , let the polygon Q_s consist of D_s extended by the vertex u_s (cf. Def-
 367 inition 3.2). Let T be a triangulation of P . We show how to map T to a triangulation
 368 T_Q of Q and to triangulations T_s of Q_s , for each s .

369 We first describe T_Q . It contains every triangle of T with all three vertices in Q . For
 370 each triangle Δ in T with two vertices on Q and one vertex on the left chain of a sink
 371 gadget D_s , we replace the vertex on D_s by l_s . Similarly, if the third vertex of Δ is on the
 372 right chain of D_s , we replace it by l'_s . For every sink s , the triangle Δ_s has one vertex

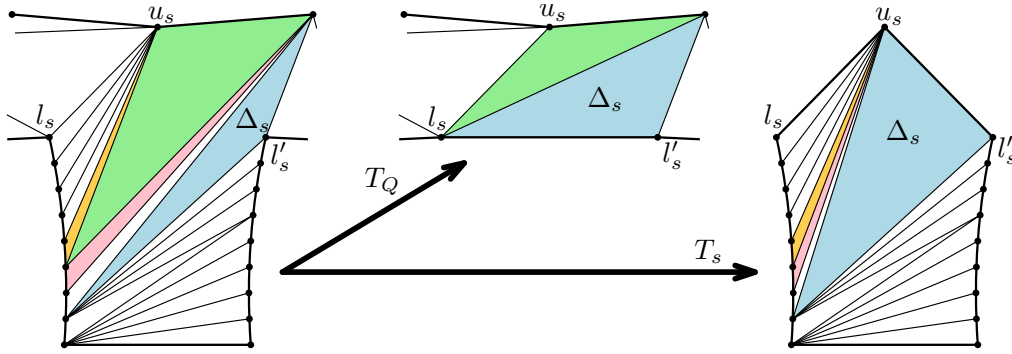


Fig. 7 Obtaining T_Q and T_s from T .

373 at a point u_i of the upper chain. In T_Q , we replace Δ_s by the triangle $l_s l'_s u_i$. No two
 374 triangles in T_Q overlap, and they cover all of Q . Thus, T_Q is indeed a triangulation of Q .

375 Now we describe how to obtain T_s , for a sink $s \in S$. Each triangle of T with all
 376 vertices on Q_s is also in T_s . Each triangle with two vertices on D_s and one vertex not
 377 in Q_s is replaced in T_s by a triangle whose third vertex is moved to u_s in T_s (note that
 378 this includes Δ_s); see Fig. 7. Again, all triangles cover Q_s and no two triangles overlap.

379 Finally, we show that a flip in T corresponds to at most one flip either in T_Q or in
 380 precisely one T_s for some sink s . We do this by considering all the possibilities for two
 381 triangles that share a common flippable edge. By construction, no two triangles that are
 382 mapped to two different triangulations T_s and T_t for sinks $s \neq t \in S$ can share an edge.

383 **Case 1.** We flip an edge between two triangles that are either both mapped to T_Q or
 384 to T_s and are different from Δ_s . This flip clearly happens in at most one triangulation.

385 **Case 2.** We flip an edge between a triangle Δ_1 that is mapped to T_s and a triangle Δ_2
 386 that is mapped to T_Q , such that both Δ_1 and Δ_2 are different from Δ_s . This results in
 387 a triangle Δ'_1 that is incident to the same edge of Q_s as Δ_1 , and a triangle Δ'_2 having
 388 the same vertices of Q as Δ_2 . Since the apex of Δ_1 is a vertex of the upper chain or z
 389 (otherwise, it would not share an edge with Δ_2), it is mapped to u_s , as is the apex of Δ'_1 .
 390 Also, the apex of Δ'_2 is on the same chain of D_s as the one of Δ_2 . Hence, the flip affects
 391 neither T_Q nor T_s .

392 **Case 3.** We flip the edge between a triangle Δ_2 mapped to T_Q and Δ_s . By construc-
 393 tion, this can only happen if Δ_s is an inner triangle. The flip affects only T_Q , because
 394 the new inner triangle Δ'_s is mapped to the same triangle in T_s as Δ_s , since both apexes
 395 are moved to u_s .

396 **Case 4.** We flip the edge between a triangle Δ of T_s and Δ_s . Similar to Case 3,
 397 this affects only T_s , because the new triangle Δ'_s is mapped to the same triangle in T_Q
 398 as Δ_s , since the two corners are always mapped to l_s and l'_s .

399 Thus, σ induces a flip sequence τ in Q and flip sequences σ_s in each Q_s so that
 400 $|\tau| + \sum_{s \in S} |\sigma_s| \leq |\sigma|$. Furthermore, each flip sequence σ_s transforms Q_s from one ex-
 401 tremite triangulation to the other. Since $|\sigma| < (d-1)^2$, Lemma 3.4 tells us that the
 402 triangulations T_s have to be transformed so that Δ_s has a vertex at u_s at some point.
 403 Moreover, by Lemma 3.3, we have $|\sigma_s| \geq 4d-4$ for each $s \in S$. Thus, τ is a flip traversal,
 404 and $|\tau| \leq |\sigma| - N(4d-4)$, as claimed. \square

405 In order to obtain a static RSA from a changing flip traversal, we use the notion
 406 of a *trace*. A *trace* is a domain on the grid. It consists of *edges* and *boxes*: an edge is
 407 a line segment of length 1 whose endpoints have positive integer coordinates; a box is
 408 a square of side length 1 whose corners have positive integer coordinates. Similar to
 409 arborescences, we require that a trace R (i) is (topologically) connected; (ii) contains
 410 the root $(0,0)$; and (iii) from every grid point contained in R there exists an x - and
 411 y -monotone path to the root that lies completely in R . We say R is a *covering trace*
 412 for S (or, R *covers* S) if every sink in S is covered by R (i.e., incident to a box or an
 413 edge in R).

414 Let τ be a flip traversal as in Lemma 4.9. By Lemma 4.7, each triangulation in τ
 415 corresponds to a chain path. This gives a covering trace R for S in the following way.
 416 For every flip in τ that extends the chain path, we add the corresponding edge to R .
 417 For every flip in τ that changes a bend, we add the corresponding box to R . Afterwards,
 418 we remove from R all edges that coincide with a side of a box in R . Clearly, R is
 419 (topologically) connected. Since τ is a flip traversal for S , every sink is covered by R .
 420 Note that every grid point p in R is connected to the root by an x - and y -monotone
 421 path on R , since at some point p belonged to a chain path in τ . Hence, R is indeed a
 422 trace, the unique *trace of* τ . Note that not only a flip traversal but any flip sequence
 423 starting with a zero-length chain path defines a trace in this way.

424 Next, we define the *cost* of a trace R , $\text{cost}(R)$, so that if R is the trace of a flip
 425 traversal τ , then $\text{cost}(R)$ gives a lower bound on $|\tau|$. An edge has cost 2. Let B be a box
 426 in R . A *boundary side* of B is a side that is not part of another box. The cost of B is 1
 427 plus the number of boundary sides of B . Then, $\text{cost}(R)$ is the total cost over all boxes

428 and edges in R . For example, the cost of a tree is twice the number of its edges, and
 429 the cost of a rectangle is its area plus its perimeter. An edge can be interpreted as a
 430 degenerated box, having two boundary sides and no interior.

431 **Proposition 4.10** *Let τ be a flip traversal and R the trace of τ . Then $\text{cost}(R) \leq |\tau|$.*

432 *Proof* Let ς_i be the sequence of the first i triangulations of τ , R_i the trace defined by ς_i ,
 433 and let κ_i be the length of the chain path for the i th triangulation. We will show by
 434 induction on i that $\text{cost}(R_i) \leq i + \kappa_i$, for $i = 1, \dots, |\tau|$. Since $\varsigma_{|\tau|} = \tau$, $R_{|\tau|} = R$, and
 435 $\kappa_{|\tau|} = 0$, this gives the desired result.

436 After the first flip, R_1 is an edge (so $\text{cost}(R_1) = 2$), and $\kappa_1 = 1$, which fulfills the
 437 invariant. Consider the i th flip. If the flip extends the chain path, the cost of the trace
 438 increases by at most 2, and the length of the chain path increases by 1, fulfilling the
 439 invariant. If the flip contracts the chain path, the trace does not change, but the length
 440 of the chain path is decreased by 1, again fulfilling the invariant. We are therefore left
 441 with the case where the flip is a chain flip. We have $\kappa_{i-1} = \kappa_i$, so we have to show
 442 that $\text{cost}(R_i) \leq \text{cost}(R_{i-1}) + 1$. We may assume that the flip adds a box B to R_{i-1}
 443 (otherwise, the cost of the trace remains unchanged). Consider the intersection of the
 444 boundary of B with the one of R_{i-1} . This intersection contains at least two elements,
 445 as the chain path is part of R_{i-1} . An edge in the intersection becomes a boundary side
 446 in R_i , reducing the cost by 1. A boundary side in the intersection vanishes in R_i , also
 447 reducing the cost by 1. Thus, adding B creates a box and at most two boundary sides,
 448 causing a cost of at most 3, but it simultaneously reduces the cost by at least 2. See
 449 the examples in Fig. 8. The overall cost increases at most by 1, and the invariant is
 450 maintained. \square

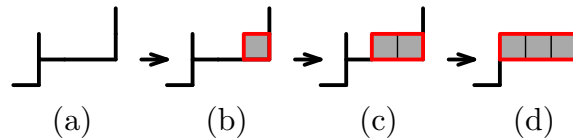


Fig. 8 Examples of how boundary sides (red) are added to a trace. To a trace of cost 16 (a) a box (gray) is added (b), which transforms two edges in boundary sides and adds two boundary sides, resulting in an overall cost of 17. The next box removes one boundary side and one edge and adds three boundary sides (c), the cost becomes 18. A box might also remove more than two elements (d), reducing the overall cost to 17.

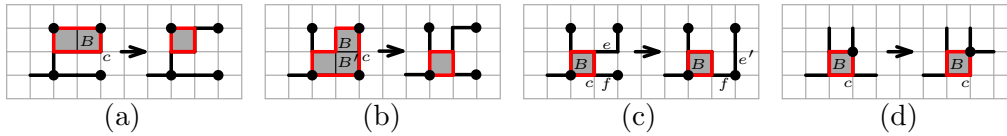


Fig. 9 Parts of traces to be modified; the boundary sides are shown in red. (a) A box that has a corner c with no incident elements can be removed. (b) Two adjacent boxes that have a shared corner c without any incident elements can be removed. (c) Replacing a single edge. (d) Sliding an edge.

451 Now we relate the length of an RSA for S to the cost of a covering trace for S , and
 452 thus to the length of a flip traversal. Since each sink is connected in R to the root by an
 453 x - and y -monotone path, traces can be regarded as generalized RSAs. In particular, we
 454 make the following observation.

455 **Observation 4.11** *Let R be a covering trace for S that contains no boxes, and let A_τ*
 456 *be a shortest path tree in R from the root to all sinks in S . Then A_τ is an RSA for S . \square*

457 If τ contains no flips that change bends, the corresponding trace R has no boxes.
 458 Then, R contains an RSA A_τ with $2|A_\tau| \leq \text{cost}(R)$, by Observation 4.11. The next
 459 lemma shows that, due to the fact that β is even, there is always a shortest covering
 460 trace for S that does not contain any boxes.

461 **Lemma 4.12** *Let τ be a flip traversal of S . Then there exists a covering trace R for S*
 462 *such that R does not contain a box and such that $\text{cost}(R) \leq |\tau|$.*

463 To prove the lemma, we investigate the structure of minimal covering traces. There
 464 exists at least one trace of cost at most $|\tau|$, namely the trace of τ . Let \mathcal{R}_1 be the set of
 465 all covering traces for S that have minimum cost. Let $\mathcal{R}_2 \subseteq \mathcal{R}_1$ be those covering traces
 466 among \mathcal{R}_1 that contain the minimum number of boxes. If \mathcal{R}_2 contains a trace without
 467 boxes, we are done, as every covering trace in \mathcal{R}_2 fulfills the requirements of Lemma 4.12.
 468 We show that this is actually the case by assuming, for the sake of contradiction, that
 469 every covering trace in \mathcal{R}_2 contains at least one box.

470 Let $R \in \mathcal{R}_2$ and suppose that R contains a box. Let B be a *maximal* box in R , i.e., R
 471 has no other box whose lower left corner has both x - and y -coordinate at least as large
 472 as the lower left corner of B . In order to prove Lemma 4.12, we need several lemmata
 473 on traces of minimum cost.

474 **Lemma 4.13** *Let B be a maximal box and let c a corner of B that is not the root $(0, 0)$.*
 475 *Then c is incident either to a sink, an edge, or another box.*

476 *Proof* Suppose there exists a corner c for which this is not the case. Note that such a c
 477 cannot be the lower left corner of B , as there has to be an x - and y -monotone path to
 478 the root. Hence, we could remove c and B while keeping the sides of B not incident to c
 479 as edges, if necessary; see Fig. 9(a). In the resulting structure, every element still has
 480 an x - and y -monotone path to the root: If c is the lower right or upper left corner, any
 481 path initially passing through c could be rerouted to pass through the corner opposite
 482 of c in B . If c is the upper right corner of B , no path is passing through c . Hence, the
 483 resulting structure would be a covering trace with smaller cost, contradicting the choice
 484 of R . \square

485 **Lemma 4.14** *Suppose B shares a horizontal side with another box B' . Let c be the right*
 486 *endpoint of the common side. Then c is incident either to a sink, an edge, or another*
 487 *box.*

488 *Proof* Suppose this is not the case. Then we could remove B and B' from R while
 489 keeping the sides not incident to c as edges, if necessary; see Fig. 9(b). This results in
 490 a valid trace that has no higher cost but less boxes than R , contradicting the choice
 491 of R . \square

492 **Lemma 4.15** *Let c be the lower right corner of B . Then c has no incident vertical edge.*

493 *Proof* Such an edge would be redundant, since c already has an x - and y -monotone path
 494 to the root that goes through the lower left corner of B . \square

495 *Proof (Proof of Lemma 4.12)* Using the Lemmata 4.13, 4.14, and 4.15, we derive a
 496 contradiction from the choice of R and the maximal box B . Note that since β is even,
 497 all sinks in S have even x - and y -coordinates. We distinguish two cases.

498 **Case 1.** There exists a maximal box B whose top right corner c' does not have both
 499 coordinates even. Suppose that the x -coordinate of c' is odd. (Otherwise, mirror the
 500 plane at the line $x = y$ to swap the x - and the y -axis. Note that the property of being
 501 a trace is invariant under mirroring the plane along the line $x = y$; in particular, the
 502 choice of B in R as a maximal box remains valid) By Lemma 4.13, there is at least
 503 one edge incident to the top right corner of B (it cannot be a box by the choice of B ,
 504 and it cannot be a sink because of the current case). Recall the slide operation for an
 505 edge in an arborescence. This operation can easily be adapted in an analogous way to
 506 traces. If there is a vertical edge v incident to c' , it cannot be incident to a sink. Thus,

507 we could slide v to the right (together with all other vertical edges that are above v
 508 and on the supporting line of v). Hence, we may assume that c' is incident to a single
 509 horizontal edge e ; see Fig. 9(c). By Lemma 4.13, the bottom right corner c of B must be
 510 incident to an element. We know that c cannot be the top right corner of another box
 511 (Lemma 4.14), nor can it be incident to a vertical segment (Lemma 4.15). Thus, c is
 512 incident to an element f that is either a horizontal edge or a box with top left corner c .
 513 But then e could be replaced by a vertical segment e' incident to f , and afterwards B
 514 could be removed as in the proof of Lemma 4.13, contradicting the choice of R .

515 **Case 2.** The top right corner of each maximal box has even coordinates. Let B be
 516 the rightmost maximal box. As before, let c be the bottom right corner of B . The y -
 517 coordinate of c is odd; see Fig. 9(d). By the choice of B , we know that c is not the
 518 top left corner of another box: this would imply that there is another maximal box to
 519 the right of B . We may assume that c is not incident to a horizontal edge, as we could
 520 slide such an edge up, as in Case 1. Furthermore, c cannot be incident to a vertical
 521 edge (Lemma 4.15), nor be the top right corner of another box (Lemma 4.14). Thus, B
 522 violates Lemma 4.13, and Case 2 also leads to a contradiction.

523 Thus, the choice of R forces a contradiction in either case. Hence, the minimum
 524 number of boxes in a minimum covering trace for S is 0. \square

525 Now we can finally complete the proof of Theorem 4.1 by giving the second direction of
 526 the correspondence.

527 **Lemma 4.16** *Let $k \geq 1$ and let σ be a flip sequence on P from T_1 to T_2 with $|\sigma| \leq$
 528 $2\beta k + (4d - 2)N$. Then there exists an RSA for S of length at most βk .*

529 *Proof* Trivially, there always exists an RSA on S of length less than $2\beta nN$, so we may
 530 assume that $k < 2nN$. Hence (recall that $\beta = 2N$ and $d = nN$),

$$531 \quad 2\beta k + (4d - 2)N < 2 \cdot 2N \cdot 2nN + 4nN^2 - 2N < 12nN^2 < (d - 1)^2,$$

532 for $n \geq 14$ and positive N . Thus, σ meets the requirements of Lemma 4.9, and therefore
 533 we can obtain a flip traversal τ for S with $|\tau| \leq 2\beta k + 2N$. By Lemma 4.12 and
 534 Observation 4.11, we can conclude that there is an RSA A for S that has length at most
 535 $\beta k + N$. By Theorem 2.1, there is an RSA A' for S that is not longer than A and that
 536 lies on the Hanan grid for S . The length of A' must be a multiple of β . Thus, since
 537 $\beta > N$, we get that A' has length at most βk . \square

538 5 Conclusion

539 In this paper, we showed NP-hardness of determining a shortest flip sequence between
540 two triangulations of a simple polygon. This complements the recent hardness results
541 for point sets (obtained by reduction from variants of VERTEX COVER). However, while
542 for point sets the problem is hard to approximate as well, our reduction does not rule
543 out the existence of a polynomial-time approximation scheme (PTAS), since a PTAS
544 is known for the RSA problem [17]. When problems that are hard for point sets are
545 restricted to simple polygons, the application of standard techniques—like dynamic
546 programming—often gives polynomial-time algorithms. This is, for example, the case
547 for the construction of the minimum weight triangulation. Our result illustrates that de-
548 termining the flip distance is a different, harder type of problem. Is there a PTAS for the
549 flip distance between triangulations of a polygon? Even a constant-factor approximation
550 would be interesting.

551 For convex polygons (or, equivalently, points in convex position), the complexity
552 of the problem remains unknown. Our construction heavily relies on the double chain
553 construction, using many reflex vertices. Does the problem remain hard if we restrict
554 the number of reflex vertices to some constant fraction?

555 References

- 556 1. Abel, Z., Ballinger, B., Bose, P., Collette, S., Dujmović, V., Hurtado, F., Kominers, S., Langerman,
557 S., Pór, A., Wood, D.: Every large point set contains many collinear points or an empty pentagon.
558 *Graphs Combin.* **27**, 47–60 (2011)
- 559 2. Aichholzer, O., Mulzer, W., Pilz, A.: Flip Distance Between Triangulations of a Simple Polygon
560 is NP-Complete. In: Proc. 29th European Workshop on Computational Geometry, pp. 115–118.
561 Braunschweig, Germany (2013)
- 562 3. Aichholzer, O., Mulzer, W., Pilz, A.: Flip distance between triangulations of a simple polygon is
563 NP-complete. In: H.L. Bodlaender, G.F. Italiano (eds.) *Algorithms - ESA 2013 - 21st Annual*
564 *European Symposium*, Sophia Antipolis, France, September 2-4, 2013. Proceedings, *Lecture Notes*
565 *in Computer Science*, vol. 8125, pp. 13–24. Springer (2013)
- 566 4. Bose, P., Hurtado, F.: Flips in planar graphs. *Comput. Geom.* **42**(1), 60–80 (2009)
- 567 5. Canny, J.F., Donald, B.R., Ressler, E.K.: A rational rotation method for robust geometric algo-
568 rithms. In: Proc. 8th Symposium on Computational Geometry (SoCG 1992), pp. 251–260 (1992)
- 569 6. Chazelle, B., Guibas, L.J., Lee, D.T.: The power of geometric duality. *BIT* **25**(1), 76–90 (1985)
- 570 7. Culik II, K., Wood, D.: A note on some tree similarity measures. *Inf. Process. Lett.* **15**(1), 39–42
571 (1982)

-
- 572 8. Edelsbrunner, H., O'Rourke, J., Seidel, R.: Constructing arrangements of lines and hyperplanes
573 with applications. *SIAM J. Comput.* **15**(2), 341–363 (1986)
- 574 9. Eppstein, D.: Happy endings for flip graphs. *JoCG* **1**(1), 3–28 (2010)
- 575 10. Hanke, S., Ottmann, T., Schuierer, S.: The edge-flipping distance of triangulations. *J.UCS* **2**(8),
576 570–579 (1996)
- 577 11. Hurtado, F., Noy, M., Urrutia, J.: Flipping edges in triangulations. *Discrete Comput. Geom.* **22**,
578 333–346 (1999)
- 579 12. Husemöller, D.: *Elliptic Curves*. Graduate Texts in Mathematics. Springer-Verlag, New York, NY,
580 USA (2003)
- 581 13. Hwang, F., Richards, D., Winter, P.: *The Steiner Tree Problem*. Annals of Discrete Mathematics.
582 North-Holland (1992)
- 583 14. Kanj, I.A., Xia, G.: Flip distance is in FPT time $O(n+k \cdot c^k)$. *ArXiv e-prints* (2014). Arxiv:1407.1525
- 584 15. Lawson, C.L.: Transforming triangulations. *Discrete Math.* **3**(4), 365–372 (1972)
- 585 16. Lawson, C.L.: Software for C^1 surface interpolation. In: J.R. Rice (ed.) *Mathematical Software III*,
586 pp. 161–194. Academic Press, NY (1977)
- 587 17. Lu, B., Ruan, L.: Polynomial time approximation scheme for the rectilinear Steiner arborescence
588 problem. *J. Comb. Optim.* **4**(3), 357–363 (2000)
- 589 18. Lubiw, A., Pathak, V.: Flip distance between two triangulations of a point-set is NP-complete. In:
590 *Proc. 24th CCCG*, pp. 127–132 (2012)
- 591 19. Pilz, A.: Flip distance between triangulations of a planar point set is APX-hard. *Comput. Geom.*
592 **47**(5), 589–604 (2014)
- 593 20. Rao, S.K., Sadayappan, P., Hwang, F.K., Shor, P.W.: The rectilinear Steiner arborescence problem.
594 *Algorithmica* **7**, 277–288 (1992)
- 595 21. Shi, W., Su, C.: The rectilinear Steiner arborescence problem is NP-complete. In: *Proc. 11th SODA*,
596 pp. 780–787 (2000)
- 597 22. Sleator, D., Tarjan, R., Thurston, W.: Rotation distance, triangulations and hyperbolic geometry.
598 *J. Amer. Math. Soc.* **1**, 647–682 (1988)
- 599 23. Trubin, V.: Subclass of the Steiner problems on a plane with rectilinear metric. *Cybernetics* **21**,
600 320–324 (1985)
- 601 24. Urrutia, J.: Algunos problemas abiertos. In: *Proc. IX Encuentros de Geometría Computacional*,
602 pp. 13–24 (2001)

603 A A Note on Coordinate Representation

604 Since it is necessary for the validity of the proof that the input polygon can be represented in size
 605 polynomial in the size of the YRSA instance, we give a possible method to embed the polygon with
 606 vertices at rational coordinates whose numerator and denominator are polynomial in N . By an additional
 607 perturbation argument we can guarantee integer coordinates whose values are polynomial in N (which
 608 slightly strengthens the result). We first introduce the general technique used for the embedding, and
 609 then give further details on how the sink gadgets are constructed (using methods similar to [19]). Finally,
 610 we explain how the construction can be transformed to integer points in general position.

611 A.1 Placing Points on Arcs

612 The main idea of the construction is to place all vertices on rational points on circular arcs. There are
 613 two large arcs where we place the vertices of the upper and the lower chain, and smaller arcs on which
 614 we place the vertices of the sink gadgets. All these circular arcs are chosen from *rational circles*, i.e.,
 615 circles that are defined by three rational points. Similarly, a *rational line* is a line through a rational
 616 point with rational slope (or, equivalently, a line defined by two rational points). It is well-known that,
 617 if one of the two intersection points of a rational line with a rational circle is a rational point, then the
 618 other intersection point is rational as well (see, e.g., [12, p. 5]). Hence, given a rational point p on a
 619 rational circle, we can obtain an arbitrary number of rational points on the circle via different rational
 620 lines through p .

621 Let us apply this for one possible way of constructing the double chain D . The construction is shown
 622 in Fig. 10 (left). We place the $\beta n + 2$ points of the lower chain on the unit circle (with center at the
 623 origin). Let ℓ_i be the line through $(-1, 0)$ with slope $1 + \frac{i}{\beta n + 2}$. For $i = 1, \dots, \beta n / 2 + 1$, we get $\beta n / 2 + 1$
 624 rational points on the upper-left quadrant of the unit circle from the intersections with this family of
 625 lines. We can do the analogous construction for points on the upper-right quadrant by choosing lines
 626 through $(1, 0)$ with a negative slope $(-1) - \frac{i}{\beta n + 2}$. In this way, we obtain the vertices of the lower chain
 627 of D . For the upper chain, we place points on the unit circle with origin $(0, 3)$ analogously. Note that
 628 line $\ell_{\beta n / 2 + 1}$ passes through $(1, 3)$, so when picking rational points on the lower-right and lower-left
 629 quadrant of the second unit circle for the upper chain, the resulting point set is indeed the vertex set of
 630 a double chain in which the line through l_0 and $u_{\beta n + 1}$ is $\ell_{\beta n / 2 + 1}$. Finally, note that all slopes used in
 631 the construction have numerators and denominators that are polynomial in N . Hence, this also holds
 632 for the coordinates of the vertices of D . Note that this is, essentially, the parametrization of the unit
 633 circle, as discussed in [5].

634 Clearly, this method is not restricted to unit circles. We now discuss the following main building
 635 block for constructing the sink gadgets. Given three rational points p_1, p_2, p_3 , we construct a circular
 636 arc on a rational circle that starts at p_1 , ends at p_2 and is completely contained inside the triangle
 637 $p_1 p_2 p_3$. Then, we choose an arbitrary number of rational points on that circular arc. This is illustrated
 638 in Fig. 10 (right). W.l.o.g, let the inner angle of the triangle at p_1 be less than or equal to the one
 639 at p_2 . Let Z be the circle through p_1 and p_2 such that the line $p_1 p_3$ is a tangent of Z . Clearly, Z is
 640 well-defined, and the arc between p_1 and p_2 is inside the triangle. The circle Z is rational. (Consider

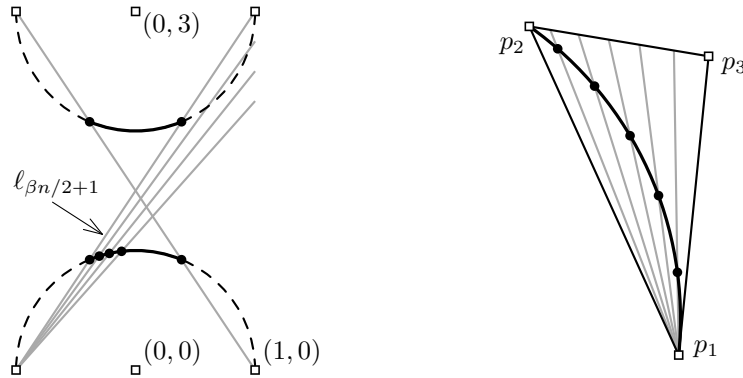


Fig. 10 Left: Construction of the main double chain D . Right: Picking points on a circular arc inside a triangle. The line p_1p_3 is tangent to the corresponding circle.

641 the line that is perpendicular to the line p_1p_3 and passes through p_1 . When mirroring p_2 with that
 642 line as an axis, the resulting point p'_2 is rational and also on Z .) We can now choose any number of
 643 rational points on the circular arc by selecting a family of lines through p_1 . To this end, we choose a set
 644 of equidistant points on the segment p_2p_3 , which, together with p_1 define this family of rational lines.
 645 Again, the numerators and the denominators are polynomial in those of p_1 , p_2 , and p_3 , and the number
 646 of points chosen.

647 A.2 Constructing Sink Gadgets

648 We now construct the sink gadgets. See Fig. 11 for an accompanying illustration. Recall that, since β is
 649 even, there are no small double chains on neighboring positions on the lower chain. Hence, for each sink
 650 we w.l.o.g. can define an orthogonal region within which we can safely draw the small double chain; we
 651 call this region the *bin* of the sink (outlined gray in Fig. 11). Consider a sink (i, j) . The vertical line
 652 bounding the left side of its bin passes through the edge $l_{j-1}l_j$ (e.g., at the midpoint of the edge), and
 653 the right side of the bin is defined analogously. (Recall that, since $\beta > 1$, there is no sink at $l_{j-1}l_j$.)
 654 Pick a rational point p_a on the boundary of the bin that is to the left of the directed line l_ju_{i-1} and to
 655 the right of the directed line l_ju_i . Similarly, choose a point p_b that is to the right of the line $l_{j+1}u_{i+1}$
 656 and to the left of the line $l_{j+1}u_i$. As an additional constraint let p_a be to the left of the line p_bu_i . Note
 657 that such points always exist, and can be easily chosen along the boundary of the bin. It remains to
 658 choose a triangular region with l_jp_a as one side in which we can place the chain of the sink gadget that
 659 contains l_j . For the second chain, the construction is analogous.

660 For the chain to be visible from u_i but not from u_{i-1} , the triangular region has to be to the left
 661 of the line $p_a u_i$, and also to the left of the line $l_j u_{i-1}$. Further, to be visible from all vertices of the
 662 other chain, it has to be to the left of the lines $p_a l_{j+1}$ and $p_b l_j$. Let x_a be the apex of the triangle that
 663 is defined by these constraints, and observe that x_a is the intersection of two of the four lines. We can
 664 now add a chain of points on a circular arc inside the triangle $l_j p_a x_a$, as described above.

665 The coordinates are rational, and since every point can be constructed using only a constant number
 666 of other points, the numerator and denominator of each point are polynomial.

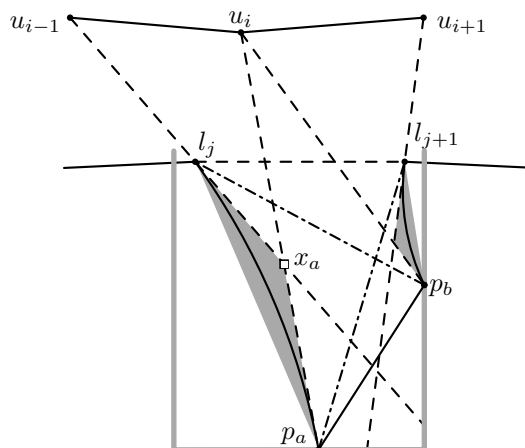


Fig. 11 Construction of a small double chain for a sink.

667 A.3 General Position and Integer Coordinates

668 The ways in which a simple polygon can be triangulated is determined by the *order type* of the vertices,
 669 i.e., the vector that indicates for each triple of vertices whether it is oriented clockwise or counterclock-
 670 wise. Up to now, we did not care whether the point set is in general position, so there might also be
 671 collinear point triples among vertices that are not directly related in the reduction. By simply multi-
 672 plying all coordinates by all denominators used, we would obtain integer coordinates with exponential
 673 values. To obtain integer coordinates bounded by a polynomial in the input size and a point set in
 674 general position, we can use the following lemma.³

675 **Lemma A.1** *Let S be a point set with rational coordinates whose numerators and denominators have*
 676 *absolute values of at most ξ . Then there is a point set S' with integer coordinates bounded by $O(\xi^2)$*
 677 *and a bijection between S and S' such that for every ordered triple of non-collinear points in S , the*
 678 *orientation of the corresponding triple in S' is the same. In particular, if S is in general position, then*
 679 *S and S' have the same order type. Further, S' can be constructed in $O(|S|^2)$ time.*

680 *Proof* Consider the set L of lines that are defined by all pairs of points of S . Choose $\ell = q_1 q_2 \in L$ and
 681 $p \in S \setminus \ell$ such that the horizontal distance v between p and ℓ is minimal among all such distances (which
 682 is non-zero as p is not on ℓ). Then v is rational, with numerator and denominator in $O(\xi^2)$. Further,
 683 our choice required $v > 0$. When multiplying all x -coordinates by $2/v$, this distance is at least 2. The
 684 basic idea is to round the x -coordinates. The crucial observation is that p has a y -coordinate that is
 685 between the ones of q_1 and q_2 , as otherwise one of q_1 and q_2 , say, q_1 , would be horizontally closer to
 686 the line through p and q_2 . For an ordered triple of points to change its orientation (from, say, clockwise
 687 to counterclockwise), the horizontal distance between the point whose y -coordinate is between those
 688 of the other two points would have to be reduced by more than 2. We can therefore safely round
 689 the x -coordinates, which, in the worst case, reduces the horizontal distance between p and ℓ by at
 690 most 1. Hence, for every non-collinear ordered triple of points in S , the orientation of the corresponding

³ The exact time bounds shown in the proof are irrelevant for the NP-hardness reduction (which even requires a different model of computation). We mention them only as they may be of general interest.

691 triple in the resulting point set is the same. We repeat the process analogously for the y -coordinates,
 692 obtaining S' .

693 The horizontal or vertical distance v can easily be found by checking all triples of points. We can
 694 improve this cubic time bound by considering the dual line arrangement \mathcal{A} of S (in which a point
 695 $p = (x_p, y_p)$ corresponds to the dual line $p^* : y = x \cdot x_p + y_p$). The dual arrangement can be constructed
 696 in quadratic time [6, 8]. The shortest vertical distance in the primal corresponds to the shortest vertical
 697 distance of a vertex and a side of a triangle defined by three dual lines. Clearly, the shortest distance
 698 can only occur inside a triangle that is not intersected by another line.⁴ Hence, we only need to test
 699 the $O(|S|^2)$ triangular cells of \mathcal{A} . □

700 Hence, if we construct the vertices with rational coordinates such that the vertices are in general
 701 position, we can apply Lemma A.1 to have all vertices on the integer grid in general position.

702 General position can easily be obtained by applying a simple technique used in [19, Appendix A].
 703 Observe first that the vertices of D are in general position. We take special care when placing the $d - 1$
 704 points of each chain of a sink gadget to not produce collinear points. Note that the final polygon P will
 705 have $|P| = 2(\beta n + 2) + 2N(d - 1)$ vertices. Instead of $d - 1$ points, we choose $2\binom{|P|}{2} + d - 1$ *candidate*
 706 *points* on the circular arc for the chain. Consider any line through two already placed points. This line
 707 intersects the circular arc in at most two points, so there are at most two candidate points that may
 708 not be points of the double chain because of that line. As there are less than $\binom{|P|}{2}$ such lines, there are
 709 always enough candidate points left for selecting the $d - 1$ points for the chain among them. Thus, the
 710 vertices we obtain are in general position.

⁴ Actually, any dual transform will do. When thinking of the rounding process as a continuous transformation, a change of the order type would involve a collapsing triangular cell of the dual arrangement, indicating a “close” point triple.